OPTIMIZATION OF DRIVE-BUNCH CURRENT PROFILE FOR ENHANCED TRANSFORMER RATIO IN BEAM-DRIVEN ACCELERATION TECHNIQUES*

F. Lemery[1], D. Mihalcea[1], and P. Piot[1,2]
[1] Department of Physics and Northern Illinois Center for Accelerator & Detector Development, Northern Illinois University DeKalb, IL 60115, USA
[2] Accelerator Physics Center, Fermi National Accelerator Laboratory, Batavia, IL 60510, USA

Abstract

In recent years, wakefield acceleration has gained attention due to its high acceleration gradients and cost effectiveness. In beam-driven wakefield acceleration, a critical parameter to optimize is the transformer ratio. It has been shown that current shaping of electron beams allows for enhanced (> 2) transformer ratios. In this paper we present the optimization of the pulse shape of the drive bunch for dielectric-wakefield acceleration.

INTRODUCTION

In collinear beam-driven acceleration technique, a "drive" electron bunch with suitable parameters propagating through a high-impedance structure or plasma medium induces an electromagnetic wake. A following "witness" electron bunch, properly delayed, can be accelerated by these wakefields. Collinear beam-driven acceleration techniques have demonstrated accelerating fields in excess of GV/m [1, 2]. The fundamental wakefield theorem [3] limits the transformer ratio – the maximum accelerating wakefield E_+ over the decelerating field E_- experienced by the driving bunch – to $\mathcal{R} \equiv |E_+/E_-| \leq 2$ for bunches with symmetric current profiles. Tailored bunches with asymmetric , e.g. a linearly-ramped, current profiles can lead to $\mathcal{R} > 2$ [4]. Achieving large transformers ratios is beneficial for beam-driven acceleration as it enables longer interaction time and increase the overall efficiency of the method; however, large values of R compromise large values of values of E_+.

Although appealing, enhancing the transformer ratio by shaping the bunch current profile has never been attempted because of the last of feasible shaping methods. Instead the transformer ratio was enhanced by using the ramped-bunch-train technique [5, 6, 7]. Over the last few years, techniques to shape the bunch on timescales below 1 picosecond have emerged; allowing new possibilities for transformer-ratio enhancement [8, 9, 10].

To understand the trade off between the peak accelerating field and transformer ratio, we explore several current profiles. In order to quantify the performance of the numerically-generated current profiles to enhance beam-driven acceleration techniques, we consider a drive bunch injected in a cylindrical-symmetric dielectric-lined waveguide (DLW) [11]. The DLW consists of a hollow dielectric cylinder with inner and outer radii a and b. The cylinder is taken to be diamond (relative electric permittivity $\epsilon_r = 5.7$); and its outer surface is contacted with a perfect conductor; see Fig. 1.

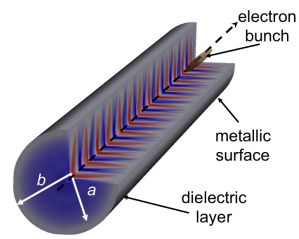

Figure 1: Geometry of the dielectric-wakefield acceleration investigated in this paper. The electron bunch passes through a dielectric cylinder producing a wakefield in the vacuum region (r $< a$). The dielectric material is located in the region $\delta = b - a$. The cylinder's outer surface is also coated with a conducting layer.

CURRENT PROFILES

The maximization of $\mathcal{R}$ has been well studied and can be achieved by making the decelerating field constant over the drive bunch as discussed in Ref. [4]. In contrast, the maximization of E_+ can be achieved by maximizing the peak peak current. This however, produces a very large E_- which effectively reduces $\mathcal{R}$. We therefore explore the relationship between E_+ and $\mathcal{R}$ for different current shapes. The six shapes considered are as follows:

- Gaussian distribution: $g(x) = \frac{1}{\sqrt{2\pi}\sigma} e^{-(z-\mu)^2/(2\sigma^2)}$, where μ and σ are the mean and root-mean-square (rms) length,
- Linearly-ramped: $g(z) = mz + b$, with m and b as parameters,
- Fourier distribution: $g(z) = \sum_{n=1}^{5} b_n \sin(nz)$ where b_n's are free parameters,

* This work was sponsored by the DTRA award HDTRA1-10-1-0051 to Northern Illinois University, and by the DOE contract DE-AC02-07CH11359 to the Fermi research alliance LLC.

- Double triangle distribution [12] as a combination of two linearly-ramped distribution parametrized by l_n and h_n, the horizontal and vertical position of the n-th vertice respectively.
- Exponential distribution: $g(z) = e^{-\alpha z}$ for $z \in [0, L]$ with α and L as parameters,
- Skewed gaussian distribution: $g(z) = \frac{2}{\omega}\phi\left(\frac{z-\xi}{\omega}\right)\Phi\left(\alpha\left(\frac{z-\xi}{\omega}\right)\right)$, where ξ is a shift, ω the characteristic length, and α the skew, $\phi(x) = \frac{1}{\sqrt{2\pi}}e^{-\frac{x^2}{2}}$, and $\Phi(x) = \frac{1}{2}\left[1 + \text{erf}\left(\frac{x}{\sqrt{2}}\right)\right]$,
- "Realistic" current achievable with longitudinal-phase-space manipulation [10] $g(z) = \int d\tilde{z} I_f^u(\tilde{z}) \exp[-\frac{(z-\tilde{z})^2}{2\sigma_u^2}]$, where $I_f^u(z) = \frac{\hat{I}_0}{\Delta^{1/2}(z)} \exp[-\frac{(a_f+\Delta^{1/2}(z_f))^2}{8b_f^2\sigma_{z,0}^2}] \times \Theta[\Delta(z)]$, with $\Delta(z) \equiv a_f^2 + 4b_f z$ and $\Theta()$ is the Heaviside function. The final current shape is therefore controlled via the parameters a_f and b_f. Here we take $\sigma_u = 0.05$.

Typical shapes associated to these functions $g(z)$ are displayed in Fig. 2. Once a set of parameters is selected, the corresponding distribution is normalized to i.e. unity as $\bar{g}(z) = \frac{g(z)}{\int_{-\infty}^{+\infty} g(z)dz}$. The bunch charge is then set to $Q = 1$ nC to yield the current profile $I(z) = Qc\bar{g}(z)$ where c is the velocity of light.

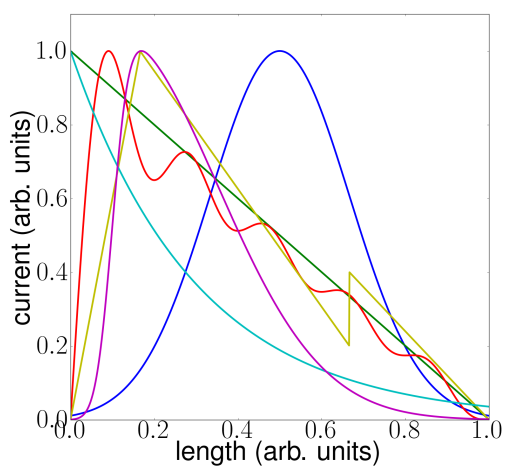

Figure 2: Shapes considered in our study: Gaussian (blue), linearly-ramped (green), exponential (cyan), Fourier (red), double triangle (yellow), and skewed gaussian (magenta). The axis are normalized to unity for clarity, e.g., the traces shown correspond to $g[z/\text{max(z)}]/\text{max[g(z)]}$.

SIMULATION METHODS

In order to explore the performances of the current profiles in beam-driven dielectric-wakefield acceleration, we considerer a diamond DLW with parameters listed in Tab. 1. Given the current profile $I(z)$, the axial electric field is computed as the integral

$$E(z) = \sum_n \int_{-\infty}^{z} I(z-\tilde{z})W_n(\tilde{z})d\tilde{z} \quad (1)$$

where $W_n(z)$ are the Green's functions associated to the nth mode; see Ref. [13]. For our calculation with limit the summation to $n = 4$ modes. Once the axial field is obtained the the decelerating field is computed as $E_- = \max[E(z)]$ for z within the bunch and $E_+ = \min[E(z)]$ for z behind the bunch.

Table 1: Parameters associated to the dielectric structure used in the wakefield simulations.

Distribution	Parameters	Units
inner radius a	165	μm
outer radius b	195	μm
relative permittivity ϵ_r	5.7	–
fundamental frequency f_0	0.83	THz

These semi-analytical simulations were imbedded in a genetic optimizer [14]. For each current profile, the associated parameters were varied. The two goals of the optimizer are to find parameters that maximize E_+ and $\mathcal{R}$.

RESULTS

Each shape was was optimized over the parameters listed above respectively. Bunch shapes with a small number of parameters (e.g. gaussian and ramped bunch) converged more quickly than more complicated shapes (e.g double triangle, skewed gaussian, "realistic" parameterization). On average, approximately 15,000 runs were done per shape. The best achieved values for $\mathcal{R}$ and E_+ are summarized in Fig. 3.

We clearly see a trade-off between $\mathcal{R}$ and E_+: as expected, current profiles resulting in large $\mathcal{R}$ are restricted to smaller values of E_+ and vice versa. The data presented in Fig. 3 was generated using a 1-nC electron bunch; increasing the charge would result in higher E_+ without affecting $\mathcal{R}$. Interestingly, none of the asymmetric shapes investigated stand out as a best candidate. A linear regression of the best cases provides an empirical limit for the maximum value of $\mathcal{R}$: $\max[\mathcal{R}] \sim 400 \times E_+^{-0.8}$. For the chosen structure parameters, value of $\mathcal{R} > 10$ are achieved with $E_+ \approx 100$ MV/m. Again, increasing the charge to, e.g., 5-nC would result in 0.5-GV/m field or alternatively could enable reaching higher transformer ratio values for 100-MV/m fields as done in Ref. [12]. In DLW-based acceleration, larger E_+ values could also be reached by reducing the aperture of the structure.

For the chosen structure parameters, value of $\mathcal{R} > 10$ are achieve with E_+ in the vicinity of 100 MV/m for 1-nC. Increasing the charge to, e.g., 5 nC would results in 0.5

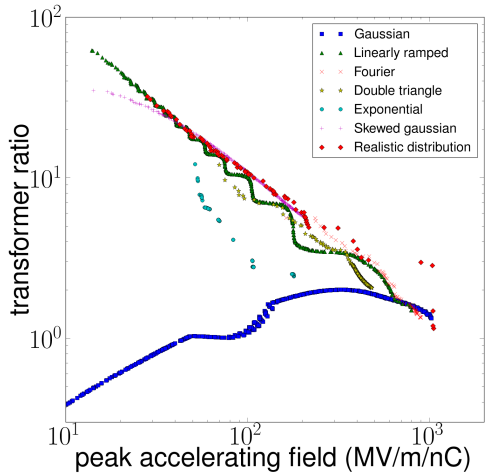

Figure 3: Trade-off curve between $\mathcal{R}$ and E_+ for the different shapes shown in Fig. 2 (with same color coding).

GV/m field or alternatively could enable reaching higher transformer ratio value for 100-MV/m fields as done in Ref. [12].

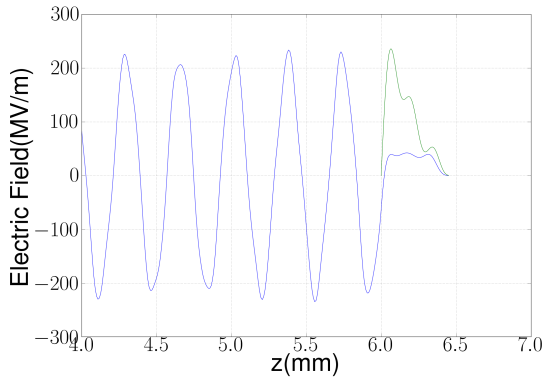

Figure 4: Fourier distribution (green trace) and associated wakefield (blue trace).

In Figures. 4 and 5 we present an example of optimized Fourier and skew-Gaussian distributions, both have $\mathcal{R} > 6$ and $E_+ > 150$ MV/m. In Fig. 5 a skewed gaussian excites a wakefield with a nice high $\mathcal{R}$. An important aspect of the skew-Gaussian distribution on this example is its ability to provide a slightly flatted accelerating field over the prospective location of a witness bunch. This latter feature, also observed for the double-triangle distribution, would reduce the energy spread imparted on the witness bunch. Finally, we present an example of wakefield generated by the "realistic" bunch in Fig. 6. Such a bunch shape is achievable using a dual-frequency linear accelerator [10] which will be used in a forthcoming experimentto demonstrate beam-driven acceleration with a enhanced transformer ratio [15, 16].

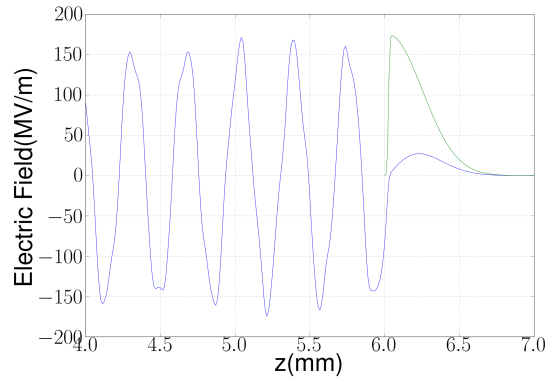

Figure 5: Skewed-Gaussian distribution (green trace) and associated wakefield (blue trace).

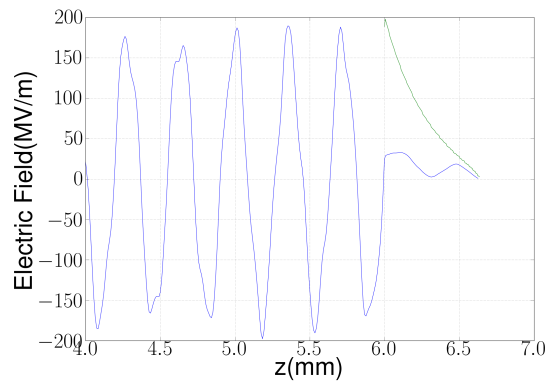

Figure 6: "Realistic" distribution (green trace) and associated wakefield (blue trace).

REFERENCES

[1] I. Blumenfeld et al., Nature **445**, 741 (2007).

[2] M.C. Thompson, *et al.*, Phys. Rev. Lett., **100**, 21 (2008).

[3] R. D. Ruth, *et al.*, Part. Accel. **17**, 171 (1985).

[4] K. L. F. Bane, *et al.*, IEEE Transactions on Nuclear Science, **NS-32**, 5 (1985).

[5] P. Schütt, *et al.*, Proc. 2nd All-Union Conference on New Methods of Charged Particle Acceleration (Springer, New York, 1989).

[6] V. Tsakanov, Nucl. Instr. Meth. **A 532**, 202 (1999).

[7] C. Jing, *et al.*, Phys. Rev. Lett. **98**, 144801 (2007).

[8] R. J. England, *et al.*, Phys. Rev. Lett. **100**, 214802 (2008).

[9] P. Piot, *et al.*, Phys. Rev. ST AB **14**, 022801 (2011).

[10] P. Piot, *et al.*, Phys. Rev. Lett. **108**, 034801 (2012).

[11] W. Gai, *et al.*, Phys. Rev. Lett. **61**, 2756 (1988).

[12] B. Jian. *et al.*, Phy. Rev. ST AB **15**, 011301 (2012).

[13] M. Rosing and W. Gai, Phys. Rev. D. **42**, 5 (1990).

[14] M. Borland and H. Shang, `geneticOptizer`, private communication (2009).

[15] F. Lemery, *et al.*, Proc. IPAC11, 2781 (2011).

[16] F. Lemery, *et al.*, these proceedings #WEEPPB01 (2012).